

A study of H.263 Traffic Modeling in Multipoint Videoconference Sessions over IP Networks

A. Drigas¹, S. Kouremenos^{1,2*}, Y. Bakopoulos¹ and V. Loumos²

1. National Center for Scientific Research "DEMOKRITOS"
Department of Technological Applications
P.O. Box 15310 Gr. Ag. Paraskevi Attikis, Greece

2. National Technical University of Athens
School of Electrical and Computer Engineering
P.O. Box 15780 Gr. Zographou, Attikis, Greece

Abstract

This manuscript is a contribution on the modeling of H.263 traffic in multipoint videoconference sessions over IP Networks. Our study includes analysis and assessment of modeling of extensive data gathered during realistic videoconference sessions between commercial H.263-compliant terminal clients (with different videoconference software packages installed). All terminal clients were communicating through a Multipoint Control Unit (software or hardware MCU) at "switched presence" mode and for comparative purposes the same typical videoconference content (a person speaking, with mild movement and occasional zoom/span) was used. Analysis of H.263 data at the frame level suggests that the traffic from the different terminals to the MCU can be represented by a stationary stochastic process with an autocorrelation function (ACF) rapidly decaying to zero and a Gamma formed marginal frame-size distribution (PDF). An accurate analysis of the H.263 traffic from all terminals (with the same visual content and different videoconference software used) shows indicative differences in ACF and PDF of different terminals' traffic and insights that no generic traffic model can be applied for all cases. Aiming at H.263 traffic modeling, accurate and conservative enough for queuing analysis and network estimation, this study discusses methods for calculating the appropriate model parameters from the observed traffic data and proposes a new technique for unconventional fitting of the PDF. Modeling results indicate the accuracy and conservativeness of the proposed models.

Keywords: H.263 traffic modeling; multipoint videoconference; MCU; queuing

1. Introduction

Videoconference traffic modeling has been extensively studied in literature and as a result a wide range of methods (linear and nonlinear) can be found. Successful traffic modeling can provide valuable insights about the resulting network load and enables a theoretical assessment of the network performance. However, the variation of videoconference session parameters (number of participants, video bit rate, frame rate) and visual contents as well as differences in implementations of video coding turn accurate video traffic modeling into a complex procedure.

Results of earlier studies as [2, 16, 3, 19, 21], concerning variable bit-rate video streams in ATM networks, indicate that the histogram of the vbr video frame sizes exhibits an asymmetric Gamma-like shape and that the autocorrelation function decays quickly (approximately exponentially) to zero. An important body of knowledge in vbr traffic modeling is the approach in [13] where the DAR(1) [9] model is introduced. Several other models have been proposed for vbr video traffic modeling such as GBAR(1) [5] and SCENIC model [6] which are generalized forms of DAR(1). GBAR model could be a solution for H.263 traffic modeling, as it was especially designed for videoconference.

On the contrary, SCENIC is oriented to full motion video and not to a typical videoconference content with no abrupt scene changes.

Newer studies of vbr video traffic modeling reinforce the general conclusions obtained by the above earlier studies by evaluating and extending the existing models and also proposing new methods for successful and accurate modeling. Of particular importance for our work is the approach in [23] where a continuous version of DAR(1) model was proposed, named C-DAR(1). The C-DAR(1) model combines an approach utilizing a discrete-time Markov chain with a continuous-time Markov chain. Furthermore, in [20], a "stuffing" method was used for grouping frames into variable frame periods. In this study, the use of movies (like Starwars), as visual content, led to frames generation with an approximate Gamma PDF (more complex when target rate was imposed) and ACF quickly decaying to zero. In [10], H.263+ coded vbr video traffic in ATM networks was studied and the authors proposed a new model called DAR(M) which is a compound DAR(1) model. The DAR(M) model analyses the number of cells in each type of macroblock (MB) of a frame separately (I-coded, P-coded and N-coded). The final model is the mean of DAR(1) models for each type of MB. For PDF modeling and correlation coefficients estimation (in the same study), the authors used the typical methods of

*Corresponding Author: Tel.: +302106503143,
Fax: +302105632910, E-mail: skourem@central.ntua.gr

DAR(1). A scene-based MPEG traffic modeling was proposed in [17]. In this study, the authors used a simple scene detection algorithm that models scene changes by a state transition matrix and the number of GOPs of a scene by a geometric distribution. A shifting level process was applied in [18] to capture the Long Range Behavior of vbr video traffic. In this study, the authors proposed a compound ACF consisting of an exponential function, in the small lag, and a hyperbolic function in the large lag region. Long range dependence, however, is an issue of no interest here as videoconference traffic has been found to be only asymptotically self-similar [7], at a time scale not affecting queuing. This fact makes the short-range dependent method of DAR(1) and extensions of it appropriate for H.263 traffic modeling. Measurement and simulation study of videoconference traffic (H.261 and H.263) in [4] indicate the influence of session parameters (codec, quality, frame rate, maximum bandwidth) on the generated traffic pattern. Again, the PDF of H.263 traffic (at the frame level) was found to be of Gamma form and the ACF was decaying quickly to zero. A normal mixture distribution for vbr video traffic was proposed in [11] instead of the Gamma-Pareto distribution that seems to perform better than the simple Gamma and lognormal distributions (although it is rather complex).

Relevant recent studies are also [14] and [15]. In [14], the authors proposed a new marginal matching technique that produces a generalized model better than GBAR and other DAR models. An AR-based analysis is performed in [15] for modeling MPEG video at GOP layer in ATM packet switching networks. GOP-based models proposed were tested with movies (like Star Wars) and seemed to perform satisfactorily.

Today, a large number of videoconference platforms exist, the majority of them over IP-based networking infrastructures and using practical implementations of H.263 standard [8] for video coding. H.263¹ is extensively used because of its suitability for transmission over low bandwidth pipes. In comparison to the previous implementation of ITU, H.261, it is generally confirmed and experimentally proved [4] that H.263 is intended to be used on links with smaller capacity (less than 64Kbps) and thus produces frames which are in the average shorter than the frames generated by H.261 applications. Concerning H.263 video codec, there are several problems of interoperability, due to the existence of different coding “flavors”. There are H.263 draft, H.263 final and H.263+ implementations. This being the case, it is of great importance to know whether the models established in literature (for H.261, H.263 and vbr video traffic modeling) are appropriate for traffic modeling of various implementations of the H.263 coding algorithm. It is a point of question whether all H.263 versions

generate similar traffic so that a common model could be applied. If not, new or alternative models should be proposed for each case. Moreover, videoconference, as a service for entertaining (video chat), educational (virtual classrooms) and communicating (through voice or sign language) purposes, is now held through Multipoint Control Units (software or hardware) that employ a centralized management for better quality of sessions. In such a case, the traffic from the clients to the MCU is highly influenced by the parameters of the possible scenarios-modes of the MCU (codec used, number of participants, video bit rate, frame rate). Most of these factors (as will be commented upon later) change the statistical characteristics of the generated traffic (studied also in [4] and [20]).

Besides studies whose subject of research was videoconference traffic, all other studies (concerning vbr and MPEG video traffic modeling) use movies as video source of their experiments (like Star Wars) that exhibit abrupt scene changes. However, the traffic pattern generated by differential coding algorithms (like those used by H.261 and H.263) depends strongly on the variation of the visual information. For videoconference, visual information should not contain abrupt scene changes, as videoconference coding algorithms were designed for a typical “head and shoulders” content (persons conversing).

Due to the above context, the research reported in this paper undertook measurements of the IP traffic generated during videoconference sessions (at “switched presence”² mode) between four commercial H.263-compliant clients that were using a different videoconference software package. At “switched presence” mode, the MCU sends to all terminals the output from one participant, designated as “currently active”. Thus, traffic from the MCU to the terminals is not complex and not of particular interest (compared to “continuous presence” where the MCU combines the signal from all terminals and sends back the output to all the participants). The experiments covered cases with both hardware and software MCU. Video source content was created realistically (a person speaking with mild movement and no abrupt scene changes) and used for all clients for statistical comparison.

It is stressed that traffic modeling in this paper focuses on queuing studies on the network performance. Thus, particular attention is paid on properties such as long-term trends in the autocorrelation and tail behavior of the frame size distribution (a matter not thoroughly examined in previous studies besides [1]).

The rest of the paper is structured as follows: section 2 discusses the videoconferencing platform employed for experimentation, describes the scenarios of the experiments and presents some basic statistical information of the measured data. Section 3 proposes

¹ Although a newer version of H.263 exists (called H.263+), it is not yet widely used and most videoconference clients do not support it.

² “Continuous presence” mode has been extensively studied in [1] for H.261 video traffic. However, the focus of our study is the H.263 traffic generated by terminal clients and not by the MCU.

methods for the modeling of the generated traffic for all cases. Finally, section 4 culminates with conclusions and pointers to further research.

2. Description of the Videoconference Experiments

The experiments of the present study were realized on two different platforms (see figures 1(a) and 1(b)). The two platforms consisted of personal computers running H.263-compliant videoconference software packages and an MCU, all networked over an IP-based LAN. Four different videoconference software packages were used: MS NetMeeting 3.0 (NM), VideoLink Pro 3.0 (VL), CuSeeMe Pro 4.0 (CU) and JoinPhone Lite (JP) and two different MCUs: CISCO IP/VC 3510 unit (Hardware) and WhitePine Meeting Point Server (Software). All experiments were held at “switched” presence mode where QCIF H.263 videos are sent by all terminals to the MCU and a QCIF video is returned back (that of the “currently active” user).

The current study examines four different factors which may influence the traffic pattern generated by the terminals. These factors are presented along with the way they are tested:

- H.263 Implementation (Use of different videoconference software package for each terminal)
- Quality of Videoconference (Use of different video bit rate in the MCU configuration)
- Target Frame Rate (Use of target frame rate in the MCU configuration - it is noted that a target frame rate was configured only for CISCO MCU as Meeting Point did not pose any restriction on it. This is a basic reason of the use of both MCUs)
- Motion of the Videoconference Content (Use of two visual contents, a high-motion and a low-motion content)

The study focuses on how the above factors influence (or not) the first order statistics of the terminal-generated H.263 traffic. The answer, as supported by the consistent evidence from the experiments results, will be discussed below.

Under the needs of the above context, three experiments were designed, two with software MCU and different session quality and one with hardware MCU. All software packages were configured with the same video parameters for all experiments (H.263-High Quality-QCIF). They did not pose any restriction on peak frame rate, except Join Phone Lite that was configured at a peak rate of 16 frames/s. A summary of the relevant quantities for each experiment is shown in Table 1. Concerning Table 1, it is noticed that JoinPhone Lite could not join the session of the hardware MCU, due to the restriction on its peak frame rate. Thus, NM was used instead for experiment 3 with a different visual content (VC-L). “VC-H” and “VC-L” stand for Video Content with High motion and Video Content with Low motion correspondingly. Both video contents are typical “head and shoulders” videos with different motion. The

two different video sources were used for NM in experiment 3 to test the influence of the content motion on the H.263 traffic pattern.

In each case, the IP packets exchanged between the terminals and the MCU were captured by traffic monitoring software (Ethereal). The collected data were further post-processed at the frame level³ by tracing a common packet timestamp. The produced sequences were used for further analysis. Some first conclusions, as supported by the experiments’ results (Table 1), arise concerning the influence of the four factors reported earlier. These are the following:

- There are some first clear indications of the statistical differences of the respective traffic patterns (although the same video settings and visual content have been used). It is already obvious that the four terminals utilize a different implementation of the H.263 video codec.
- The quality of the videoconference session (different MCU video bit rate used) - as clearly indicated in experiments 1 (300/300Kbps) and 2 (100/100Kbps) - influence the first order characteristics of all terminals besides JP (obviously due to the existence of a peak frame rate).
- The target frame rate is of no great importance for the traffic pattern (a small irregularity exists in the frame sizes histogram, as will be commented upon later). Most terminals are not influenced by the MCU frame rate except terminal NM that tends to send frames at a higher rate (30 frames/s) when no target frame is set (experiments 1 and 2) while it sends at a lower frame rate (15 frames/s) in the case of experiment 3.
- The motion of the video content seems to influence the variance of the traffic pattern, a fact that implies a larger periodicity (lower complexity) in the traffic signal (as remarked in experiment 3 by the comparison of the variance of NM (VC-H) and NM (VC-L)). This leads to the conclusion that variance is a measure of the amount of motion of the videoconference content.

Generally, it is noted that terminal VL sends video at a higher bit rate than terminals CU and NM while the slowest is terminal JP (apparently because of the frame rate restriction in its own configuration). Regarding frame sizes, NM⁴ and JP produce smaller frames than VL and CU. It may also be observed that the values of the bit rate achieved are in all cases much lower than the respective maximum specifications of the MCU settings, reflecting the fact that the content of the videoconference did not exhibit dramatic scene changes, frequent zooms

³ It is important to note, here, that the analysis of previous studies at GOP or MB level has been examined and found to provide only a typical smoothing in the sample data (that could be easily performed by a typical ‘box’ smoothing method). Analysis at the frame level offers a realistic view of traffic and is better for queuing studies.

⁴ From now on, we will refer to the terminals JP, VL, CU, NM as JP, VL, CU and NM correspondingly.

or other such effects. The next section will analyze the H.263 traffic of each terminal separately, proposing the corresponding traffic model and commenting more thoroughly upon the influence of the above factors.

3. Analysis of the video data sequences

Analysis of the H.263 traffic from all terminals to the MCU, for both experiments, confirms the general body of knowledge that literature has formed concerning videoconference traffic. In brief, the sequence of frame sizes from a terminal can be represented as a stationary stochastic process, with an autocorrelation function quickly decaying to zero and a marginal frame-size distribution of approximately Gamma form. All frame-size distributions except NM are Gamma-like (with a heavier tail⁵) and very asymmetrical (this can be seen in other studies of H.263 traffic too [4]). These general characteristics remain invariant for all experiments.

In checking for stationarity each frame sequence corresponding to a terminal was split in a moderate number of windows (ten) and then the empirical density function for the frame size was calculated from the sample in each window. These windows were found to be very much alike, property suggesting that the sequence is stationary. This is in accordance with the study in [1] where stationarity was found to apply for H.261 traffic. Thus, there is no point in further analyzing towards this point.

3.1. Autocorrelation Function Analysis

As can be seen in the graphs of the ACF fitted models (see figures 2(a), 2(c), 2(e), 2(g), 2(i) and 2(j)), the ACF of H.263 traffic seems to decay quickly (almost exponentially). Strong correlations in the ACFs of JP and NM (figures 2(a), 2(g), 2(i) and 2(j)) (implying periodicities in the traffic pattern) are attributed to the similarities (temporal redundancy) that exist between sequential video frames. The comparison of the experimental results showed that the ACF of H.263 traffic is not strongly influenced by the parameters of the videoconference session (quality and frame rate). Nevertheless, the ACF is different for each terminal, a fact obviously caused by the different implementations of H.263.

To be more specific, the ACFs of VL and CU (figures 2(c), 2(e)) have an almost similar behavior, a fact that indicates the statistical resemblance of the two traffic patterns (implying similarities in the implementation of the H.263 codec of the two videoconference software packages). A strong periodicity every 160 lags can be seen in the ACF of JP (figure 2(a), maybe suggesting that during the session, JP is periodically sending I frames at regular intervals. Even

stronger correlations appear in the ACF of NM (figure 2(g), 2(i) and 2(j)) with long-range implications.

The Low-motion Video Content, “VC-L”, used in experiment 3 for NM, caused a larger periodicity in the ACF (see figure 2(j) compared to figure 2(i)). The results of the ACF analysis (graphs and fitted models) will be presented for each software terminal in experiment 1, for NM (VC-H and VC-L) in experiment 3 and numerical values of the fitted models will be given for all experiments.

To find the most accurate fitting model for the ACF of H.263 traffic, three different methods, reported in literature, were used. The first two were proposed for modeling H.261 terminals traffic in multipoint videoconference at “continuous presence” [1]. The third one is an AR-based approach proposed in [12] that estimates the parameters and eigenmodes of AR models of arbitrary order. In our study the particular method was used to estimate the parameters of the correlation coefficients of the AR(1) and AR(2) models⁶. More analytically, the methods used are the following:

1. A weighted sum of two geometric terms [1]

$$\rho_k = w\lambda_1^k + (1-w)\lambda_2^k, \text{ with } |\lambda_2| < |\lambda_1| < 1 \quad (1)$$

2. A geometrically damped sinusoid [25] of the form:

$$\rho_k = \frac{\lambda_k \cos(\theta_k + \psi)}{\cos \psi} \quad (2)$$

3. AR(1) and AR(2) models:

$$\text{AR(1): } X_n = w + \alpha_1 X_{n-1} + C \quad (3)$$

$$\text{AR(2): } X_n = w + \alpha_1 X_{n-1} + \alpha_2 X_{n-2} + C \quad (4)$$

Methods (1) and (2) were tested with a least squares fit to the autocorrelation samples for the first 500 lags. Method 3 returns least squares estimates of the intercept vector w , of the coefficient matrices α_1 , α_2 , and of the noise covariance matrix C . All models were compared against the samples over a wider range of lags (up to 5000) to verify that they are capable of capturing the long-term trends of the ACF decay. Numerical values for the results appear in Table 2, while the graphs of the fitted models are compared to the sample ACFs in figure 2. The most dominant model for all cases is the Compound Exponential Fit as it is able of capturing the long-term trends of the ACF better than the other models (see figures 2(b), 2(d), 2(f) and 2(h)). The damped sinusoid (of similar behavior as in [1]) did not fit well (decayed much faster than the sample ACF) and thus is not depicted. Only in case of NM, where very strong correlations exist, it produced a satisfying fit (see figures

⁵ Tail behavior is a matter of great importance that affects queuing and will be examined thoroughly during analysis.

⁶ Although literature reports that AR(2) [13] or even of higher order AR(p) models [24] produce a better match than AR(1) models, AR(1) seems to perform well for H.263 traffic (as will be commented upon later).

2(g), 2(i) and 2(j)). AR(1) performed satisfactorily for VL and CU where AR(2) failed to fit (see figures 2(c) and 2(e)). On the contrary, AR(2) was better in cases of JP and NM where AR(1) failed (see figures 2(a) and 2(g)). It is insighted that AR(1) performs well in traffic patterns with no strong correlations (such as ACFs of VL and CU) while AR(2) is better for cases where periodicities exist (ACFs of JP and NM).

Taking into account that the long-term decay rate is the most important factor for queuing, it is evident that a proper model for fitting the autocorrelation function of H.263 traffic is the Compound Exponential Fit. In fact, what matters is the autocorrelation coefficient λ_1 in (1) as it tends to capture the long-term behavior of the ACF. The retention of this model is further verified by previous studies [1, 13] for videoconference traffic where values of λ_1 were found to be near 0.99 (see Table 2 for numerical values of λ_1). This being the case, further study towards new models is of no point.

3.2. Probability Distribution Function Analysis

Now, we may proceed to the analysis of the PDF of the traffic patterns' frame sizes which is one of the main points of the current study. In actuality, all density distributions seem to fit a gamma-like shape with a heavy tail and asymmetry. This is less obvious in the case of NM whose PDF is symmetrically bell-shaped (see figures 5(d), 5(e), 5(f)) (fact confirmed by a previous study of H.261 NM traffic [1]). On the contrary, the PDFs of JP, VL and CU are asymmetrical (see for example figures 3(g), 6(g) and 7(h)). In the analysis to follow, the Gamma density function will be used to fit the empirical PDFs.

$$f(x) = \frac{1}{\Gamma(p)} \frac{1}{\mu} \left(\frac{x}{\mu}\right)^{p-1} e^{-\frac{x}{\mu}}, \mu, p > 0, x \geq 0,$$

$$\Gamma(p) = \int_0^{\infty} u^{p-1} e^{-u} du \quad (5)$$

To achieve this, three previously known methods and a class of new methods were tried. The older ones were used for modeling H.261 traffic from terminals NM to the MCU in [1] while the new methods are based on a class of methods of moments estimators for the Gamma density, presented recently in [22]. More explicitly, the first three methods are the following:

1. MOM (Methods of moments). When the mean, m , and the variance, v , of the data sample are known, the method of moments produces estimates for the shape and scale parameters of the Gamma distribution:

$$p = \frac{m^2}{v} \text{ and } \mu = \frac{v}{m}$$

2. LVMAX. The LVMAX method relates the histogram's peak to the location at which the Gamma density achieves its maximum and to the value of this

maximum. The values of the shape and scale parameters are derived from:

$$p = 2\pi x^* f^{*2} + 1 \text{ and } \mu = \frac{1}{2\pi x^* f^{*2}}$$

where f^* is the unique maximum of the histogram density at x^* .

3. C-LVMAX. The third method is an application of the LVMAX method to the self convolution of the histogram. In this method:

$$p = \frac{2\pi x^* f^{*2} + 1}{2} \text{ and } \mu = \frac{1}{2\pi x^* f^{*2}}$$

As will be commented upon later, the above methods were tried and, except the conventional MOM method, did not provide a satisfactory fit in most cases. Thus, new methods had to be tried. The class of methods of moments estimators studied in [22] is a new body of knowledge in statistical science and (to the best knowledge of these authors) has never been tested for video traffic modeling. The members of this family are very easy to compute, relative to the maximum likelihood estimation or its commonly used approximation. More specifically, this method is a class of moment estimators (a vector θ_k of values for p and μ):

$$\theta_k = (p_k, \mu_k)^T \text{ with } \mu_k = \frac{m}{p_k}, k \geq 0$$

If $x = \{x_1, x_2, \dots, x_n\}$ is the vector of the data sample (frame sizes) and vector $x_k = \{x_1^k, x_2^k, \dots, x_n^k\}$ then the values for p and μ parameters of the Gamma function are:

$$p_k = \frac{mm_k}{k^{-1} Sx_k, x}, k > 0$$

$$p_k = \frac{m}{S \ln x, x}, k = 0$$

where m is the mean of x , m_k the mean of x_k and Sx, x_k the covariance of vectors x and x_k . The flexibility of this method is evident as for various values of k ($k > 0$) new values for the shape and scale parameters are computed and as a result a different fitting method is tested. From now on, in the current study, this method will be referred to as $K = \text{'value of } k\text{'}$ (for example $K=0, K=2, K=3$). As will be proved later, this method has been tried as an unconventional fitting method (although sufficiently simple) due to its ability to capture accurately the tail⁷ behavior of the PDF.

After extensive testing, we concluded that the MOM, $K=0$ and $K=3$ models are the most conservative (with respect to queuing behavior) and dominant for all

⁷ The distribution tail, by containing the probabilities of events corresponding to large frames, thus high bit rates, is a critical aspect to capture in a queuing model. Neglecting it may cause wrong calculations in buffer overflow estimations.

terminals. Especially, K=3 model has the advantage of capturing very well the PDF tail, a fact that makes it suitable for queuing analysis. Modeling analysis and evaluation will be presented with five methods (MOM, LVMAX, C-LVMAX, K=0 and K=3). The numerical results from the application of the above parameters-matching methods in the data appear in Table 3.

Modeling evaluation has been made with the following method: The sample and model quantiles are plotted (Q-Q plot) to test fitting accuracy. The sample quantiles derive from the PDF (cumulative distribution) of the sample and the model quantiles from the Incomplete Gamma Function $f_{inc}(x/\mu, p)$ of the corresponding model where:

$$f_{inc}(x, p) = \frac{1}{\Gamma(p)} \int_0^x e^{-t} t^{p-1} dt \quad (6)$$

and $\Gamma(p)$ derives from (5).

The Q-Q plots of the above method refer to cumulative distributions (i.e. probabilities of not exceeding a threshold). Thus, the tail behavior for the fit is indicated by the neighborhood of quantiles around 1. If the model's quantiles are lower than the sample quantiles in that neighborhood, the model is considered to be conservative (with respect to queuing). For more detail around that neighborhood, the complementary PDF is plotted together with the complementary Gamma function in the large frames region (tail).

This method gives valuable indications about the tail behavior of each model (tendency of the model to move to "high bandwidth" states) and a measure of their conservativeness concerning queuing.

In the following paragraphs, PDF modeling will be performed applying the above methods. Modeling results, commented for each case separately, lead to conclusions about the suitable models.

3.2.1. PDF analysis of terminal JoinPhone Lite

The probability distribution functions of the traffic generated by JP were found to be strongly asymmetrical (see figure 3(g) and 3(h)). Both traffic patterns of JP (experiment 1 and 2) were statistically identical reflecting the fact that there is no influence of the videoconference session parameters. Analysis performed for experiments 1 and 2 (results only for experiment 1 are depicted) showed that only MOM and K=0 models provided a satisfactory fit of the PDF (see figures 3(a), 3(d)). On the contrary LVMAX and C-LVMAX (figures 3(b), 3(c)) did not perform well. The model K=3, although being conservative in the large frames region (tail), declines considerably in the small frames region (figure 3(e)). The complementary density plot confirms the conclusions of the q-q plots and indicates the tail dominance of the models (see figure 3(f)). PDF and Gamma models for MOM and K=0 are depicted in figures 3(g) and 3(h) for experiments 1 and 2

correspondingly (as reported previously, terminal JP did not join the videoconference session of experiment 3).

3.2.2. PDF analysis of terminal NetMeeting

The frame size histograms of NM were found to be symmetrical enough compared to the other terminals. In experiment 1, the absence of a target frame rate caused a greater than usual irregularity in the small frames region as shown in figures 4(h) and 4(i). In a lower video bit rate session (experiment 2), the frame size histogram consisted mostly of the small frames contribution and as a consequence, the PDF was more narrow and tall (see figure 5(d)). More explicitly, in experiment 1, models MOM, C-LVMAX, K=0 and K=3 were found to be the most dominant (see figures 4(a)-(e)). MOM, C-LVMAX and K=0 are conservative whereas K=3 fits very accurately the PDF tail as shown by the Complementary density in figures 4(f) and 4(g). The same analysis in experiment 2 for NM showed that C-LVMAX performed better than K=0 while K=3 did not fit satisfactorily (see figures 5(a)-(c)). Experiment 3 analysis led to similar conclusions with experiment 1. MOM, C-LVMAX and K=3 models were found to be the most dominant for both cases of visual content used (VC-H and VC-L). The PDF with the best fitted models are plotted for experiments 2 and 3 in figures 5(d)-(f).

It is evident by the above results that the MCU session parameters (frame rate, video bit rate) and the motion of the visual content, although they change the shape of the PDF, do not influence dramatically the performance of the theoretical models.

3.2.3. PDF analysis of terminal Video Link Pro

Analysis of the histograms of the frame sizes for all the experiments for VL reflects clearly the non-influence of the session parameters (frame rate, video quality). In all cases, the PDFs of VL exhibit a similar asymmetrical bell-like shape (see figures 6(g), 6(i) and 6(j)). Thus, modeling results will be presented for the first experiment and PDFs will be given only for experiments 2 and 3 with the fit of the most dominant models. Q-q plots in figures 6(a)-(e) prove that the most conservative and well-fitted models are again MOM, K=0 and K=3 (see figure 6(h) for the fitted PDF plot). LVMAX and C-LVMAX do not perform well (C-LVMAX for the first time was found to be non conservative, figure 6(c)). Although MOM and K=0 models seem to perform better, K=3 model is more tail dominant as depicted in figures 6(e) and 6(f). Figures 6(g), 6(i) and 6(j) reflect the statistical resemblance of the traffic patterns generated by VL in all experiments.

3.2.4. PDF analysis of terminal CuSeeMe Pro

The similar analysis for CU proved that VL and CU have statistical similarities. Modeling results are the same for both implying a similar implementation of H.263. Conclusions are the same for all experiments and

thus full results will be presented again for the experiment 1. Figures 7(a)-(f) reflect the fact that MOM, K=0 and K=3 models are the most dominant. Figures 7(g)-(j) depict the PDF plots with the best fitted models.

3.3. A proposal for full modeling and further queuing analysis

C-DAR(1) model [23], the Continuous-time version of the approach of DAR(1) [13] can be directly applied for full modeling and analytic treatment of H.263 traffic. This model produces a sequence of frame sizes according to the transitions of a continuous time Markov Chain, of the form:

$$P_{cdar} = f(P_{dar} - I)$$

where $f = \frac{\ln \rho}{(\rho - 1)} T$, $P_{dar} = \rho I + (1 - \rho) Q$ from DAR(1)

where T is the frame rate of H.263 traffic, I is the identity matrix, ρ is the autocorrelation coefficient at lag-1 and Q is a rank-one stochastic matrix with all rows equal to the probabilities resulting from the negative binomial density corresponding to the Gamma fit for the frame size distribution.

Autocorrelation coefficient ρ should be chosen according to the parameter λ_1 of the model (1) (see Table 2) and the elements for the rows of Q should be determined through the Gamma fit produced by the most dominant model of each case (see Table 4 for a summary of the proposed models).

4. Conclusions

This manuscript was a modeling assessment of H.263-encoded traffic in multipoint videoconference sessions over IP Networks. The modeling results showed that H.263 terminal traffic was stationary and seemed to possess a rapidly decaying autocorrelation function and a Gamma-formed marginal distribution. Realistic experiments with terminals using a different implementation of H.263 codec that joined sessions with different parameters (frame rate, video bit rate) were held. The extensive analysis of the video traffic from the terminals to the MCU indicated that although the experiment parameters influence the traffic pattern, generic (though unconventional) models can capture conservatively their statistical trends. Although the correlations of H.263 traffic are more complex than a simple geometric term, careful choice of the decay rate allows the construction of a conservative approximation. Modeling of the distribution of frame sizes indicated that only three models MOM, K=0 and K=3 can be applied for all cases (with respect to queuing). Especially, K=3 model is tail-dominant in most cases and as a result a good solution for a generalization of DAR(1) model.

Further study will include queuing and simulation study of the discussed models (with C-DAR(1) as full model) in new experiments with various combinations of scenarios, visual content and H.263 implementations. Study of the traffic produced by the MCU in

“continuous presence” (H.263-encoded) is also a subject of future research.

Acknowledgements

The authors would like to thank Dr K. Kontovasilis for his constructive comments on improving this work.

References

- [1] C. Skianis, K. Kontovasilis, A. Drigas, and M. Moatsos, Measurement and Statistical Analysis of Asymmetric Multipoint Videoconference Traffic in IP Networks, *Telecommunications Systems* (2003), Volume 23, Issue 1. pp. 95-122.
- [2] H. S. Chin, J. W. Goodge, R. Griffiths, and D. J. Parish, Statistics of video signals for viewphone-type pictures, *IEEE JSAC* (1989), 7(5):826-832.
- [3] D. M. Cohen and D. P. Heyman, Performance modeling of video teleconferencing in ATM networks, *IEEE Trans. Circuits Syst. Video Technol.* (1993), 3(6):408-422.
- [4] K. Dolzer, W. Payer, On aggregation strategies for multimedia traffic, *Proceedings of the 1st Polish-German Teletraffic Symposium* (2000), Dresden.
- [5] D.P. Heyman, The GBAR source model for VBR videoconferences, *IEEE/ACM Trans. Networking* (1997), 5: 554-560.
- [6] M.R. Frater, J.F. Arnold. & P. Tan, A new statistical model for traffic generated by VBR coders for television on the broadband ISDN, *IEEE Trans. Circuits and Syst. for Video Technology* (1994), 4: 521-526.
- [7] A. Erramilli, O. Narayan, and W. Willinger, Experimental queueing analysis with long-range dependent packet traffic, *IEEE/ACM Trans. Networking* (1996), 4(2):209-223.
- [8] Video Coding for low bit rate communication, Recommendation H.263 (1998), Article number E13923.
- [9] P.A. Jacobs and P.A.W.Lewis, Time series generated by mixtures, *J. Time Series Analysis* (1983), vol. 4, no. 1, pp. 19-36.
- [10] G. Sisodia, L. Guan, M. Hedley, S. De, A New Modeling Approach of H.263+ VBR Coded Video Sources in ATM Networks, *RealTimeImag(6)*(2000), No. 5, pp. 347-357.
- [11] W.C. Poon and K.T. Lo, A refined version of M/G/ ∞ processes for modeling VBR video traffic, *Computer Communications* (2001), vol.24, no.11, pp.1105-1114.
- [12] A. Neumaier, T. Schneider, Estimation of parameters and eigenmodes of multivariate autoregressive models, *ACM Transactions on Mathematical Software (TOMS) archive* (2001), Volume 27, Issue 1, Pages: 27 - 57.
- [13] D. P. Heyman, A. Tabatabai, and T. V. Lakshman, Statistical analysis and simulation study of video teleconference traffic in ATM networks, *IEEE*

- Trans. Circuits Syst. Video Technol. (1992), 2(1):49–59.
- [14] L. Yan-ling, W. Peng, W. Wei-ling, A Steady Source Model for VBR Video Conferences, International Conference on Information Technology: Computers and Communications, IEEE (2003), Las Vegas, Nevada p. 268.
- [15] A. A. Alheraish and S. A. Alshebeili, AR-based quadratic modeling for GOP MPEG-encoded video traffic in ATM networks, Computer Communications (2003), In Press, Corrected Proof.
- [16] R. Kishimoto, Y. Ogata, and F. Inumaru, Generation interval distribution characteristics of packetized variable rate video coding data streams in an ATM network, IEEE JSAC (1989), 7(5):833–841.
- [17] S. J. Yoo and S. D. Kim, A new multi-level statistical model for variable bit rate MPEG sources over ATM networks and its performance study, Computer Communications (2001), Volume 24, Issues 3-4, Pages 296-307.
- [18] H. Ahn, J. Kim, S. Chong, B. Kim, B. D. Choi, A Video Traffic Model Based on the Shifting-Level Process: the Effects of SRD and LRD on Queueing Behavior, INFOCOM (2000): 1036-1045.
- [19] B. Maglaris, D. Anastassiou, P. Sen, G. Karlsson, and J. D. Robbins, Performance models of statistical multiplexing in packet video communications, IEEE Trans. Commun. (1988), 36(7): 834–843.
- [20] F. H. P. Fitzek and M. Reisslen, MPEG-4 and H.263 Video Traces for Network Performance Evaluation, Telecommunications Networks Group Technical Report (2000) (<http://www-tnkn.ee.tu-berlin.de/research/trace/trace.html>).
- [21] M. Nomura, T. Fujii, and N. Ohta, Basic characteristics of variable rate video coding in ATM environment, IEEE JSAC (1989), 7(5):752–760.
- [22] D. P. Wiens, J. Cheng, N. C. Beaulieu, A class of moments estimators for the two-parameter Gamma family, Pak. J. Statist (2003), Vol. 19(1) pp 129-141.
- [23] S. Xu, Z. Huang, and Y. Yao, An analytically tractable model for video conference traffic, IEEE Trans. Circuits Syst. Video Technol. (2000), 10(1):63–67.
- [24] N.D. Doulamis, A.D. Doulamis, G.E. Konstantoulakis, G.I. Stassinopoulos, Efficient Modeling of VBR MPEG-1 Coded Video Sources, CirSysVideo(10) (2000), No. 1, pp. 93.
- [25] D. R. Cox and H. D. Miller, The Theory of Stochastic Processes, Chapman & Hall (1965).

Table 1. Summary of relevant quantities for each experiment
(VC-H=Video Content with High motion, VC-L=Video Content with Low motion)

Experiment	1				2				3			
MCU	WhitePine Meeting Point (Software)				WhitePine Meeting Point (Software)				CISCO MCU 3510 (Hardware)			
Software of Terminal Client	JP	NM	VL	CU	JP	NM	VL	CU	NM	NM	VL	CU
Video Source	VC-H	VC-H	VC-H	VC-H	VC-H	VC-H	VC-H	VC-H	VC-H	VC-L	VC-H	VC-H
MCU Frame Rate (Frames/s)	-				-				15			
MCU Video Bit Rate Send/Received (Kbits/s)	300/300				100/100				300/300			
Parties	4				4				4			
Experiment Duration (s)	3600				3600				3600			
Video Frames	31745	107972	41260	48884	31750	94654	38096	17437	54302	54242	38215	45768
Video Bit Rate (Kbits/s)	50	172	283	178	50	54	125	72	170	178	252	189
Frame rate (Frames/s)	9	30	11	14	9	26	11	5	15	15	11	13
Average Frame Size (Bytes)	713	715	3082	1640	716	256	1482	1859	1407	1480	2964	1855
Variance (Bytes ²)	300690	76779	3041900	1789900	307960	9765	1419300	2842600	135450	76310	2822100	2949600

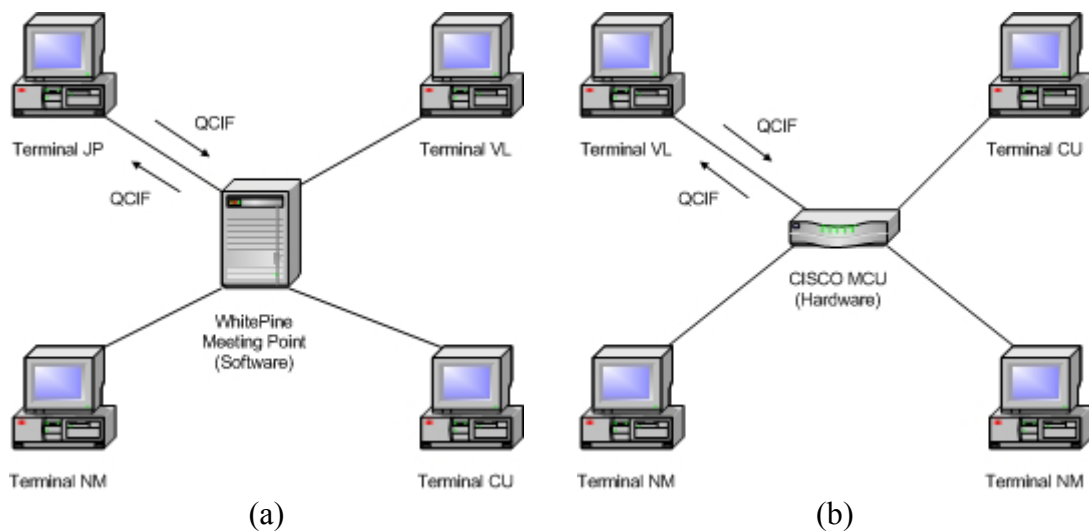


Figure 1. Testbed topologies
(JP=Join Phone Lite, VL = Video Link Pro, NM=NetMeeting, CU=CuSeeMe)

Table 2. Model parameters fitted to sample ACF
(The symbol “-” is used when the model failed to converge, *Exp*=Experiment)

<i>Exp</i>	1												
	Compound Exponential Fit			Dumped Sinusoid Fit			AR(1)			AR(2)			
	$\rho_k = w\lambda_1^k + (1-w)\lambda_2^k$			$\rho_k = \lambda^k \cos(\theta_k + \psi) / \cos\psi$			$X_n = w + \alpha_1 X_{n-1} + C$			$X_n = w + \alpha_1 X_{n-1} + \alpha_2 X_{n-2} + C$			
	w	λ_1	λ_2	λ	θ	ψ	w	α_1	C	w	α_1	α_2	C
JP	0.1058	0.9972	0.6803	0.1355	6.2832	4.7124	0.0297	0.4854	0.00091641	0.0177	0.4853	0.2001	0.0007129
NM	0.0008	0.9999	0.4288	0.2972	1.957	-1.329	0.0002154	-0.2809	0.00002492	0.0002336	-0.0974	-0.0839	0.000018642
VL	0.1144	0.997	0.759	0.2024	-6.283	1.5708	0.0025	0.8695	0.000041826	0.0004708	1.2107	-0.2372	0.000012335
CU	0.1822	0.9861	0.6143	0.1319	6.2832	4.7124	0.0056	0.6814	0.00041838	0.0001146	1.1021	-0.1286	0.000018573
<i>Exp</i>	2												
JP	0.0992	0.9972	0.6801	-	-	-	0.0293	0.4619	0.001	0.019	0.4431	0.2018	0.00085667
NM	0.0013	0.9996	0.4584	0.2295	1.9973	-1.383	0.0018	-0.2193	0.000085027	0.0013	0.2564	0.0313	0.000051467
VL	0.0811	0.9985	0.8044	0.3881	6.2728	1.8212	0.0155	0.7295	0.00014596	0.0031	1.1671	-0.2255	0.000015599
CU	0.793	0.7283	0.9985	-	-	-	0.0401	0.7177	0.00022243	0.0067	1.1108	-0.1606	0.000034146
<i>Exp</i>	3												
VL	0.0977	0.9972	0.7435	-	-	-	0.0174	0.675	0.00015733	0.0025	1.2185	-0.2685	0.00068922
CU	0.8414	0.644	0.9782	0.7457	18.85	4.7134	0.0018	0.6359	0.00031755		0.9784	-0.0463	0.000044459
NM (VCH)	0.0222	0.9963	0.525	0.0307	3.1386	-1.571	0.013	-0.153	0.00074	0.014	-0.3218	0.0578	0.000018346
NM (VCL)	0.0052	0.9975	0.4712	0.3796	1.634	-1.216	0.0037	-0.1564	0.00010112	0.0044	-0.089	-0.1489	0.000026151

Table 3. Gamma parameters for the various fitting methods applied to the terminals' data

<i>Exp</i>	1									
	MOM		LVMAX		C-LVMAX		K=0		K=3	
	p	μ	p	μ	p	μ	p	μ	p	μ
	JP	1.69	421.51	5.56	83.09	2.36	223.98	2.67	267.29	0.74
NM	6.66	107.33	13.71	66.19	7.94	102.78	5.44	131.52	8.46	84.58
VL	3.12	987	7.69	250.21	4.32	623.82	4.02	765.75	2.03	1521.8
CU	1.5	1091.4	2.53	444.62	1.5	970.59	1.98	828.29	1.04	1580.5
<i>Exp</i>	2									
JP	1.66	430.39	6.24	76.47	2.44	214.69	2.67	267.87	0.66	1082.5
NM	6.73	38.1	21.74	13.41	12.96	21.43	7.51	34.12	2.43	105.59
VL	1.55	958.02	4.79	182.78	2.8	473.35	2.19	677.14	1.04	1418.2
CU	1.22	1529.1	2.24	500.3	1.05	1523.3	1.53	1216.3	1.01	1846.9
<i>Exp</i>	3									
NM (VC-H)	14.62	96.27	24.34	66.5	15.23	94.36	12.87	109.37	16.92	83.15
NM (VC-L)	28.7	51.56	61.41	25.94	40.34	38.41	25.4	58.27	32.52	45.51
VL	3.11	952.27	8.73	219.92	4.47	606.52	4.04	734.07	2.02	1468.1
CU	1.17	1589.9	3.14	394.37	1.27	1174.2	1.68	1107.5	0.84	2213.7

Table 4. Summary of Modeling Conclusions

<i>Terminal</i>	<i>Proposed Gamma Model</i>
JP	MOM, K=0
NM	MOM, C-LVMAX, K=0, K=3
VL	MOM, K=0, K=3
CU	MOM, K=0, K=3

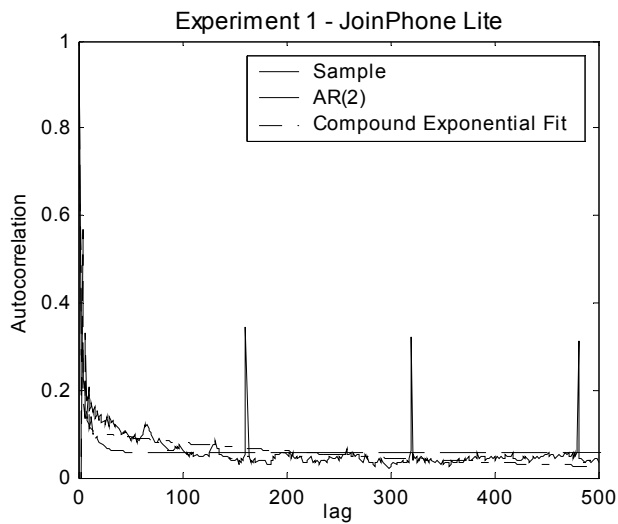


Fig. 2(a)

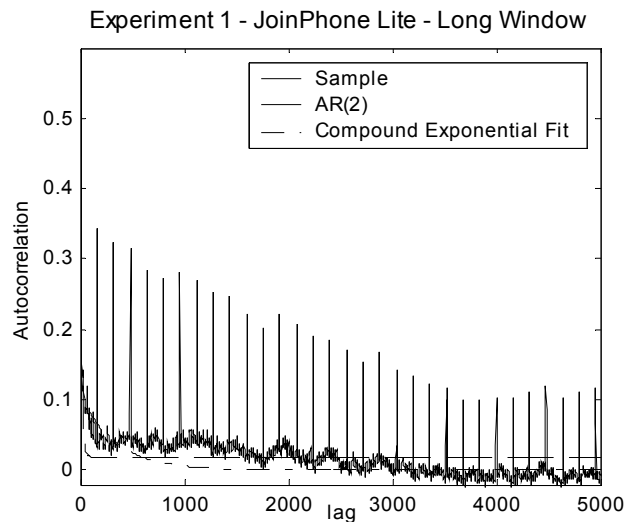


Fig. 2(b)

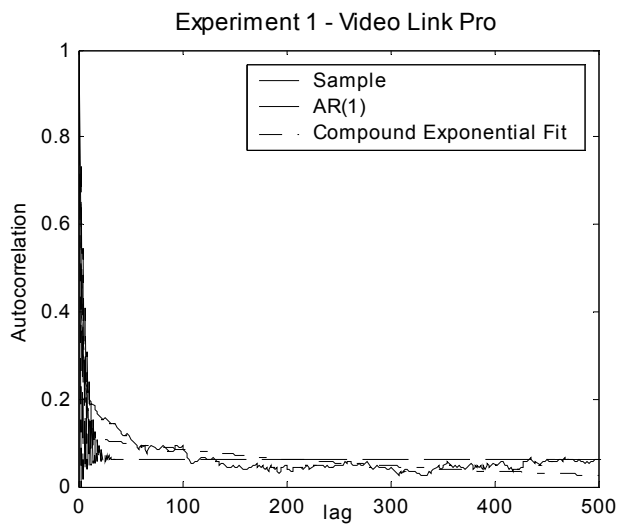


Fig. 2(c)

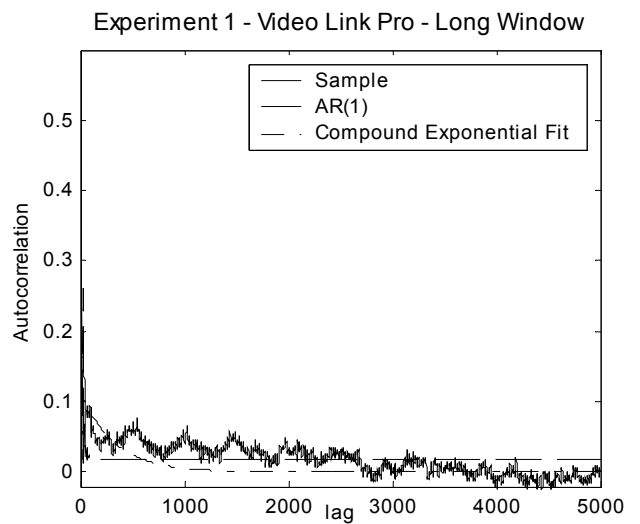


Fig. 2(d)

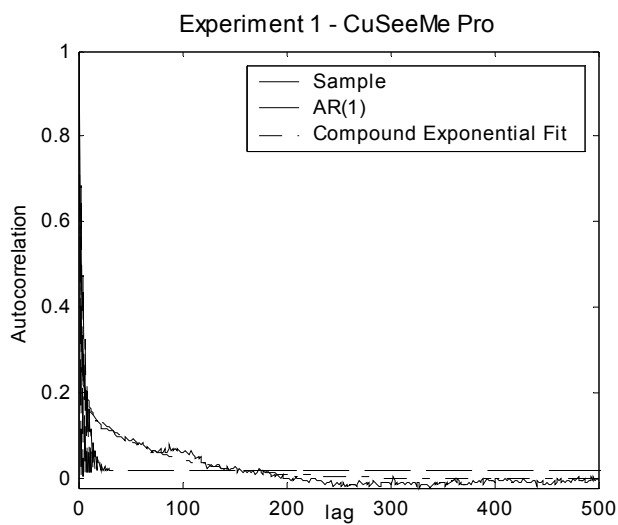


Fig. 2(e)

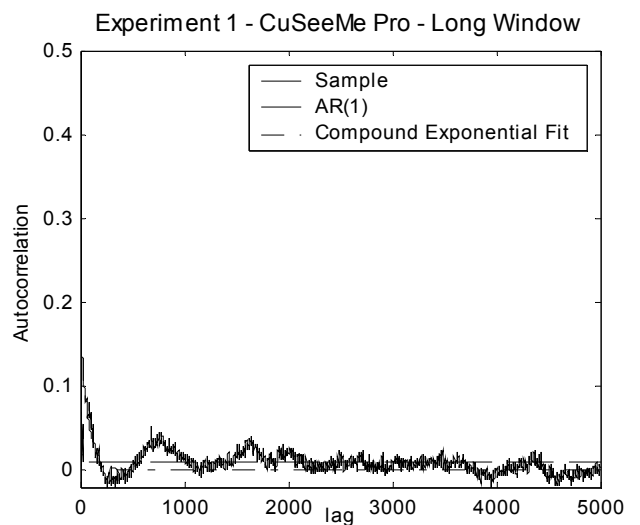


Fig. 2(f)

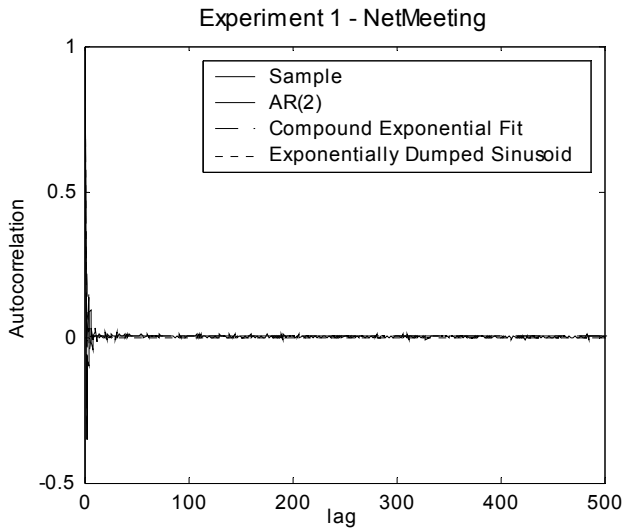


Fig. 2(g)

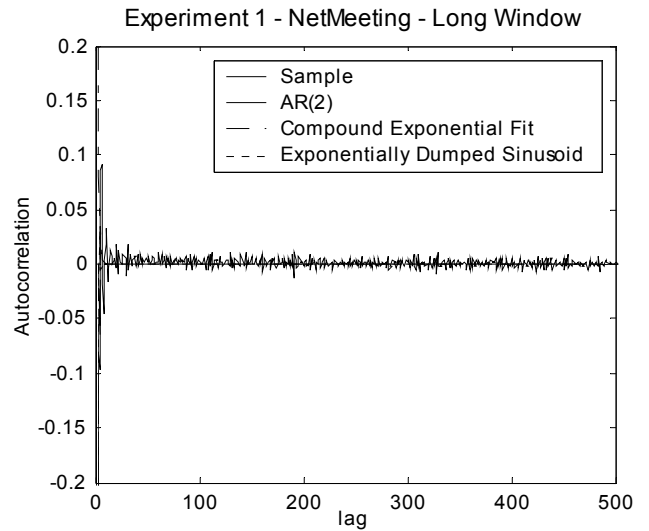


Fig. 2(h)

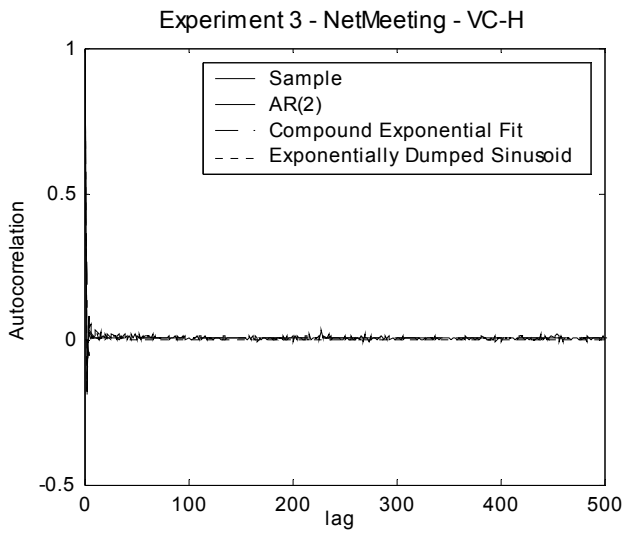


Fig. 2(i)

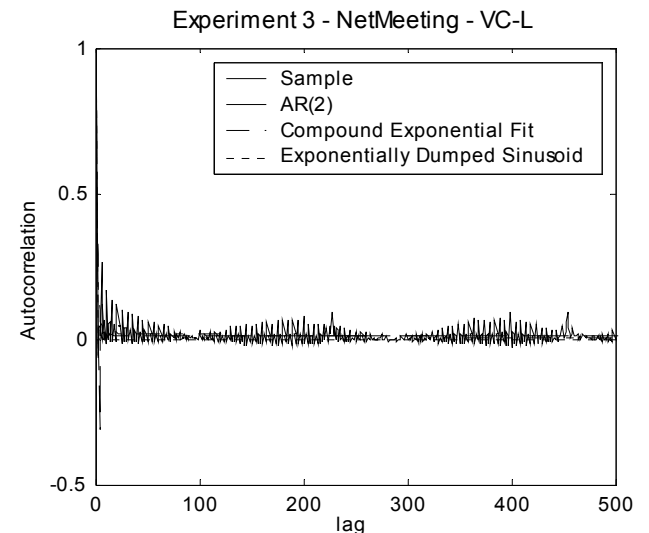


Fig. 2(j)

Figure 2. Autocorrelation Graphs and fitted models for H.263 traffic from terminals

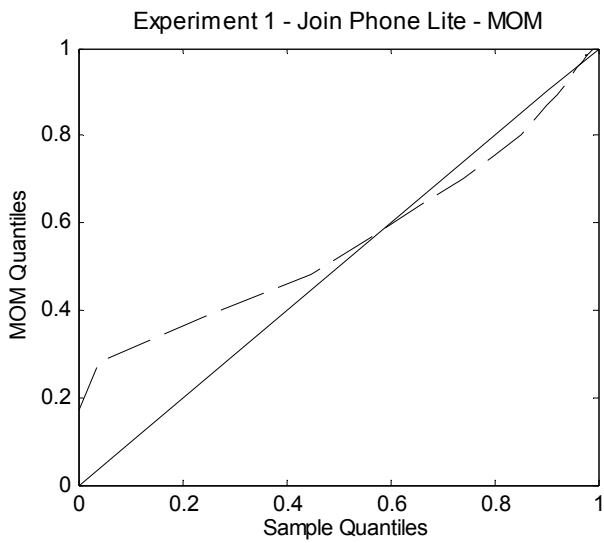


Fig. 3(a)

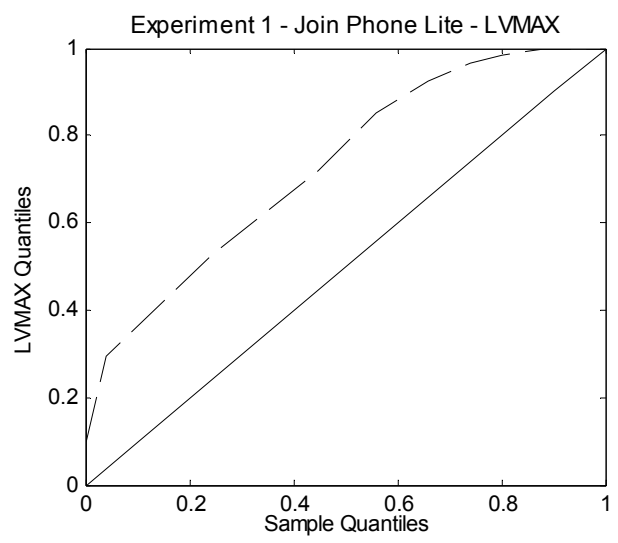


Fig. 3(b)

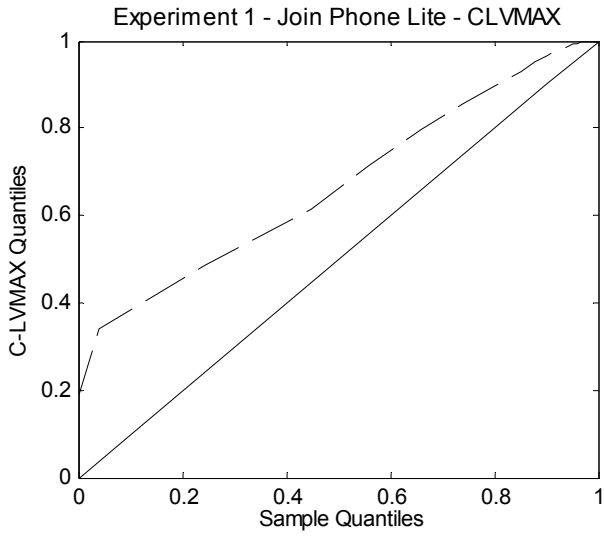


Fig. 3(c)

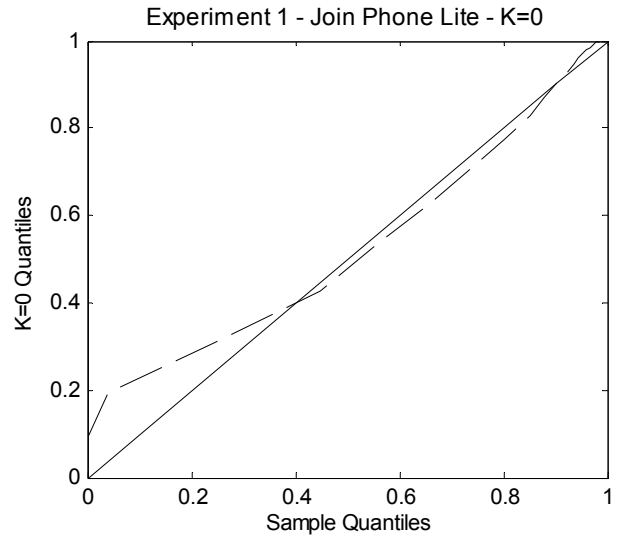


Fig. 3(d)

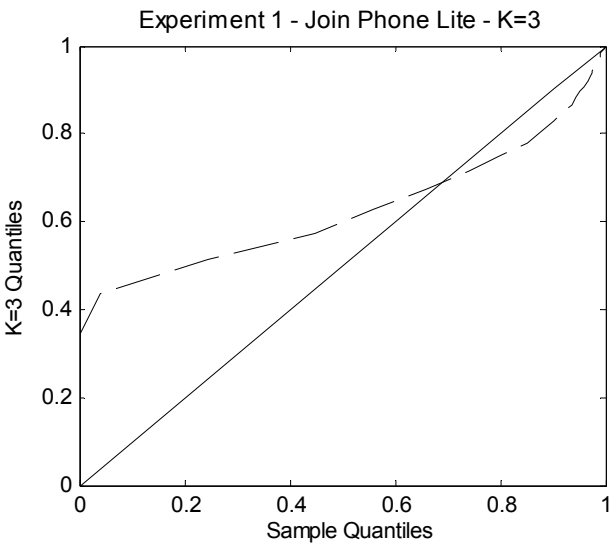


Fig. 3(e)

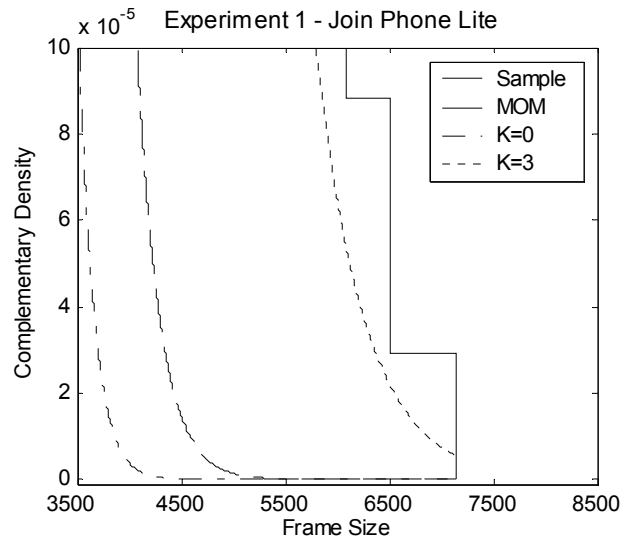


Fig. 3(f)

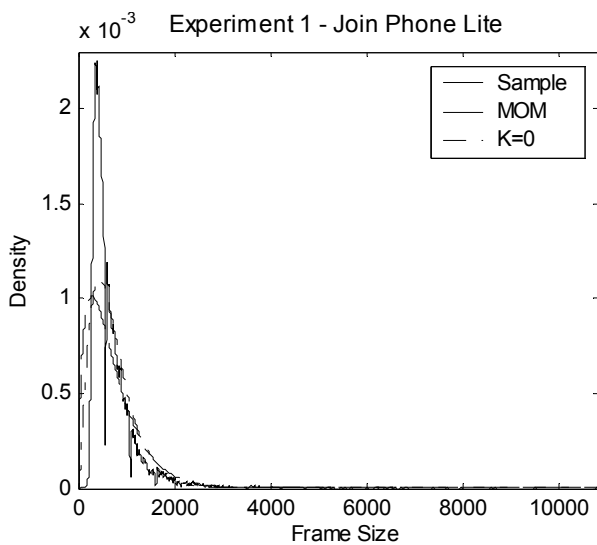


Fig. 3(g)

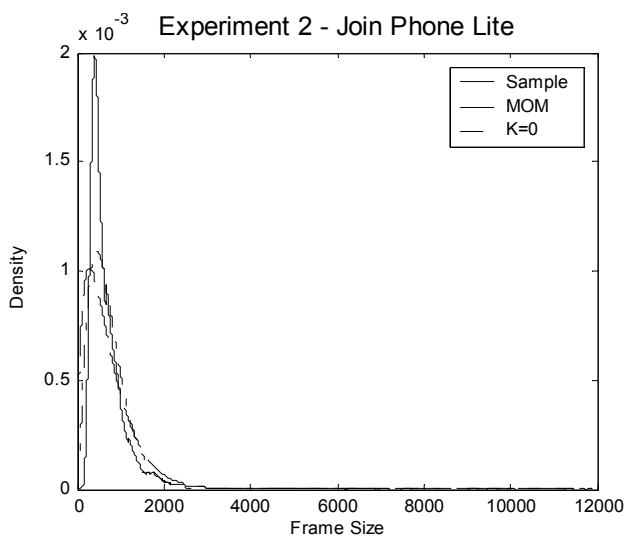


Fig. 3(h)

Figure 3. Frame size histograms-Gamma models, q-q plots and complementary probability functions for terminal JP in Experiment 1

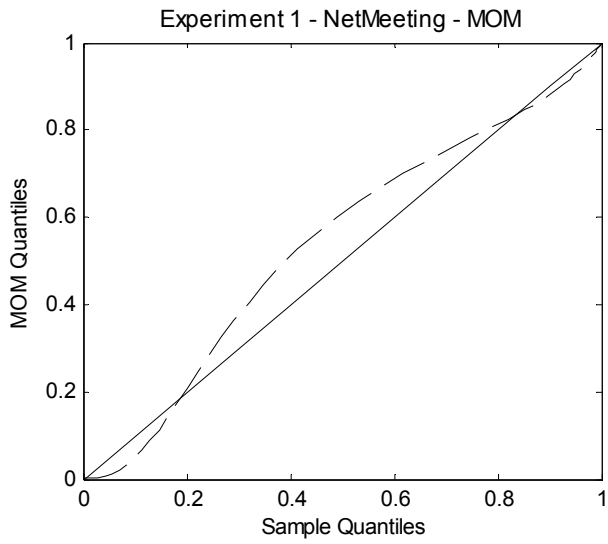


Fig. 4(a)

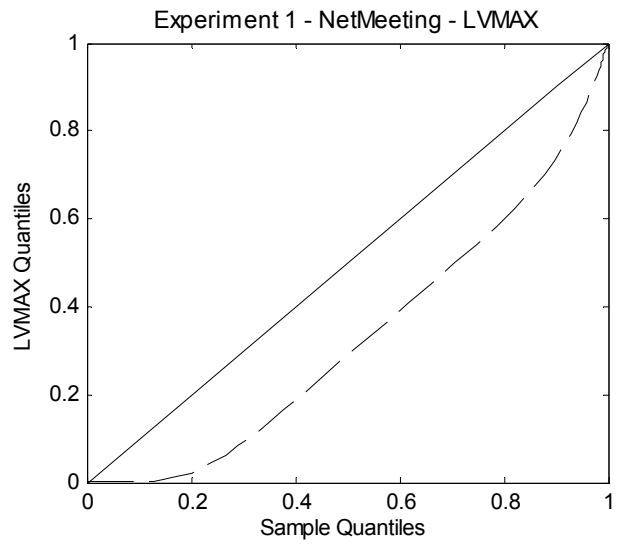


Fig. 4(b)

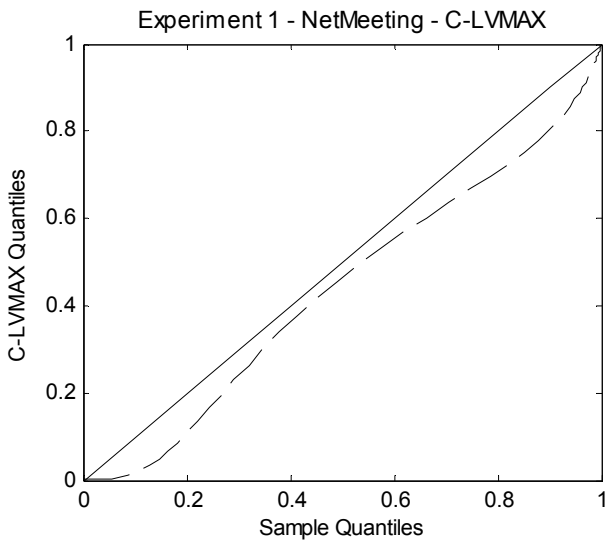


Fig. 4(c)

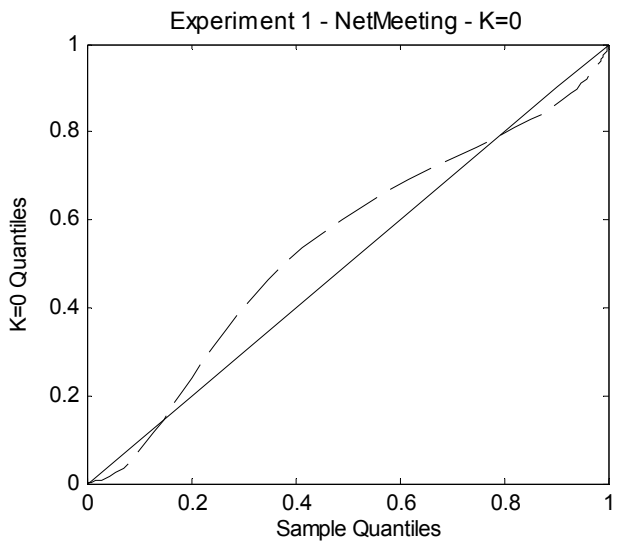


Fig. 4(d)

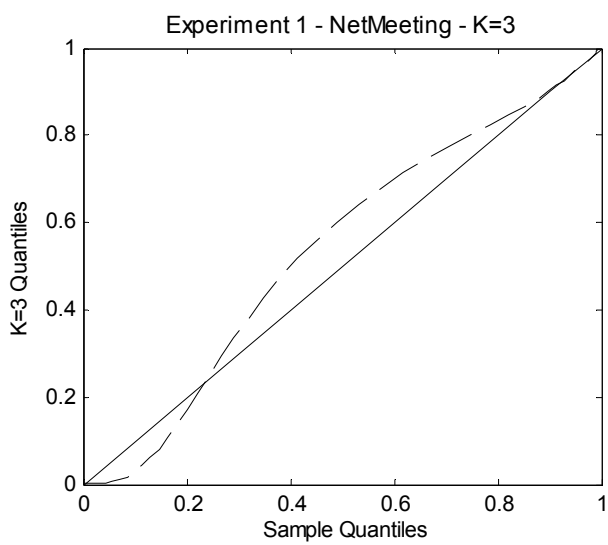


Fig. 4(e)

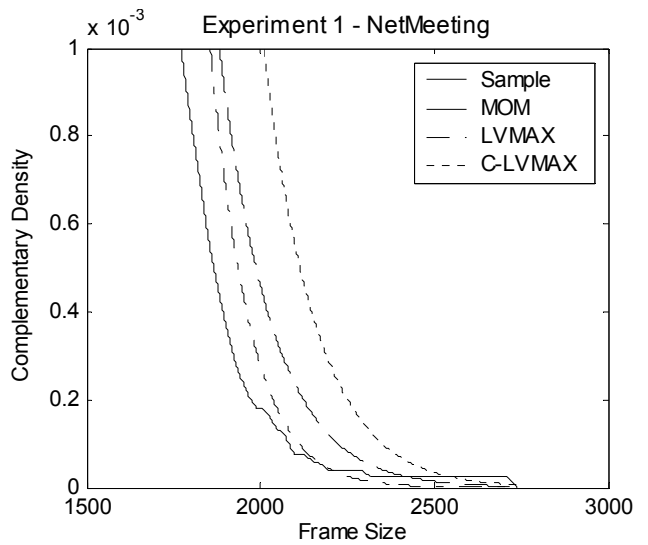


Fig. 4(f)

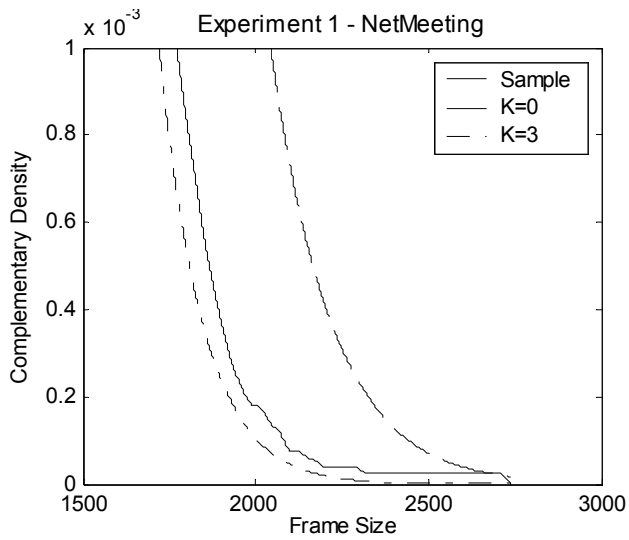


Fig. 4(g)

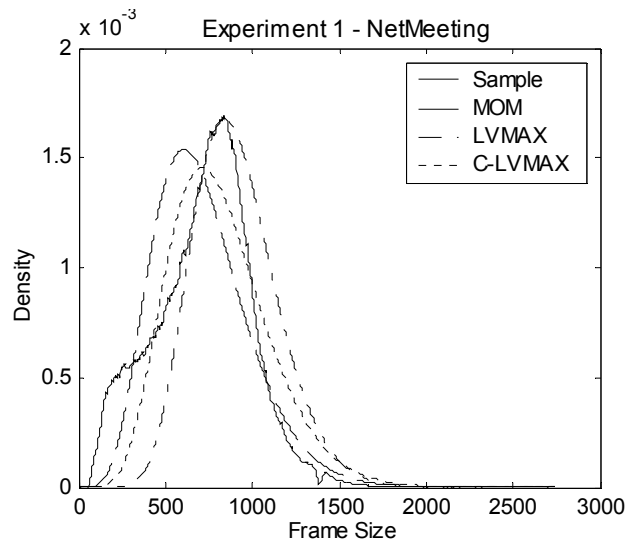


Fig. 4(h)

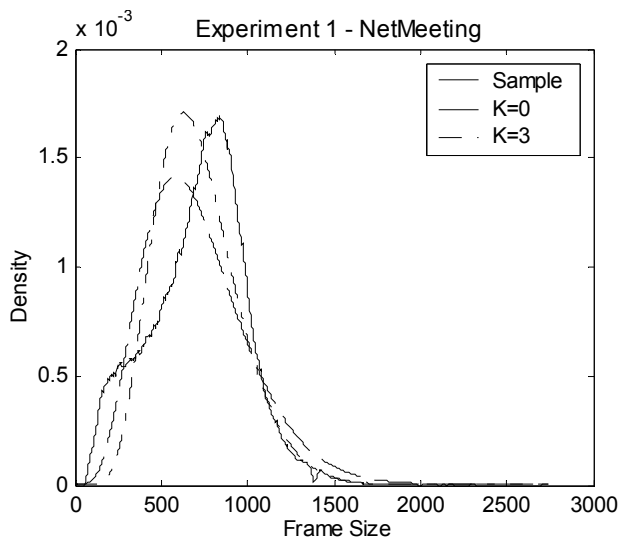


Fig. 4(i)

Figure 4. Frame size histograms-Gamma models, q-q plots and complementary probability functions for terminal NM (Experiment 1)

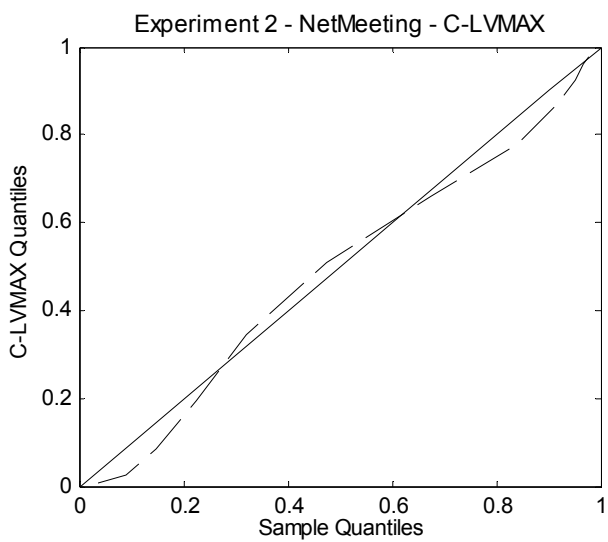


Fig. 5(a)

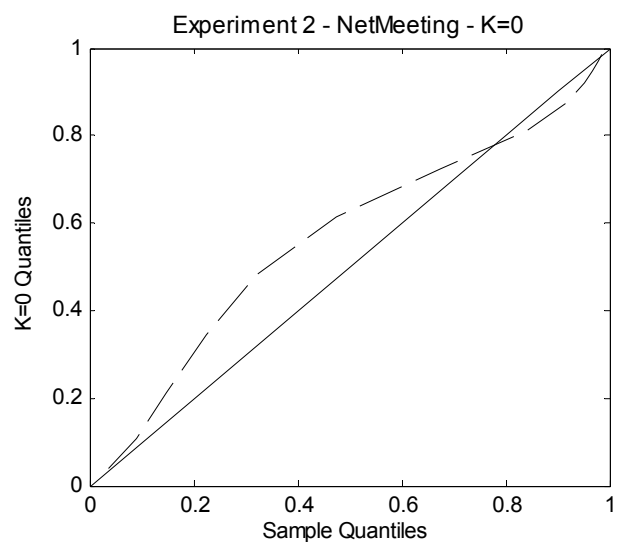


Fig. 5(b)

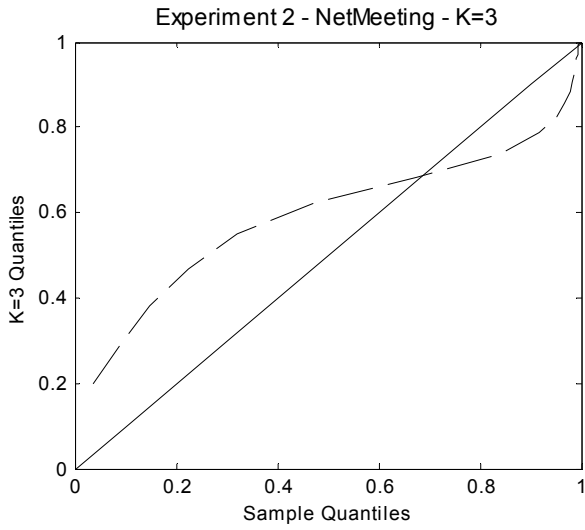


Fig. 5(c)

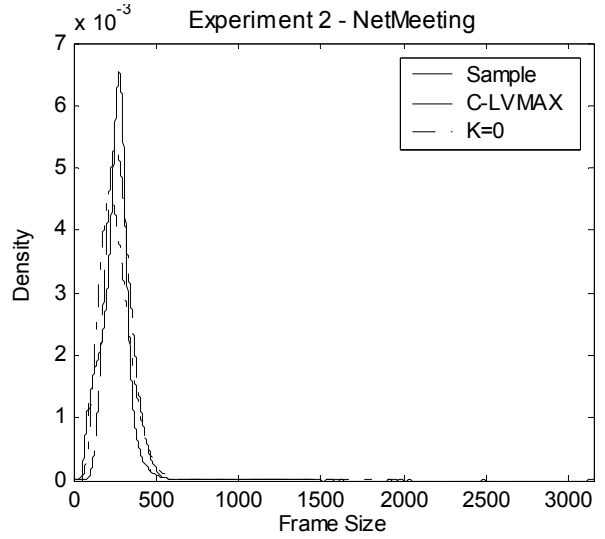


Fig. 5(d)

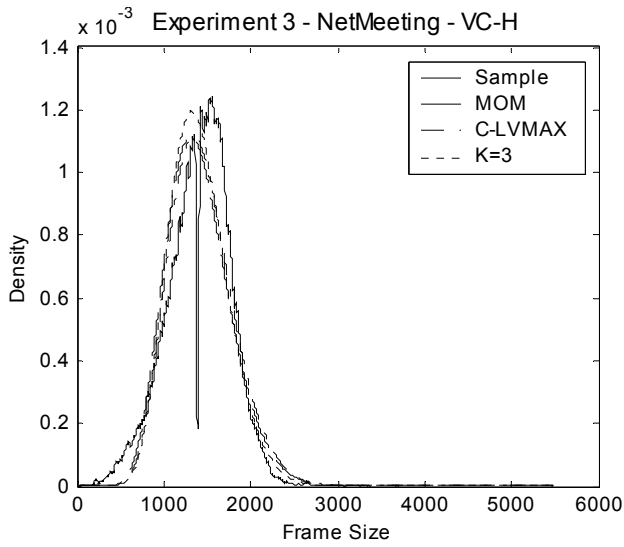


Fig. 5(e)

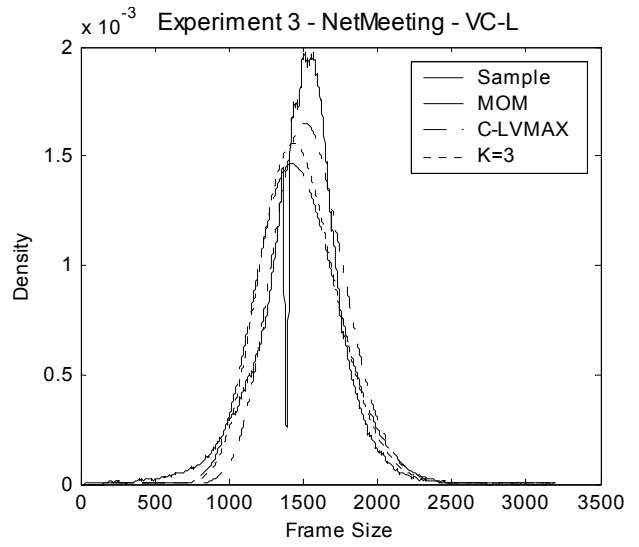


Fig. 5(f)

Figure 5. Frame size histograms-Gamma models, q-q plots and complementary probability functions for terminal NM (Experiments 2 and 3)

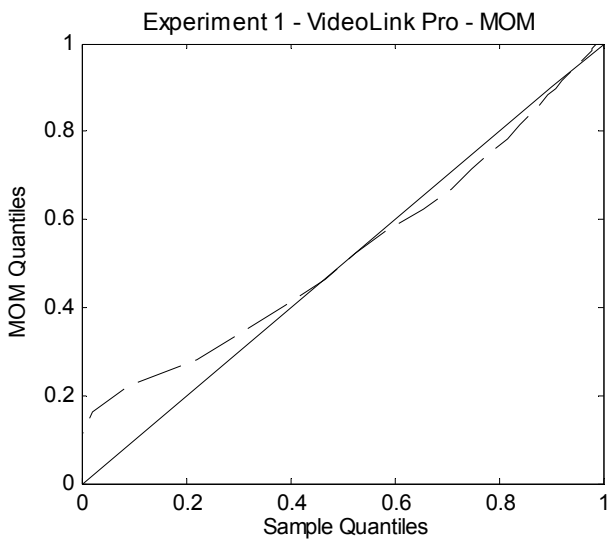


Fig. 6(a)

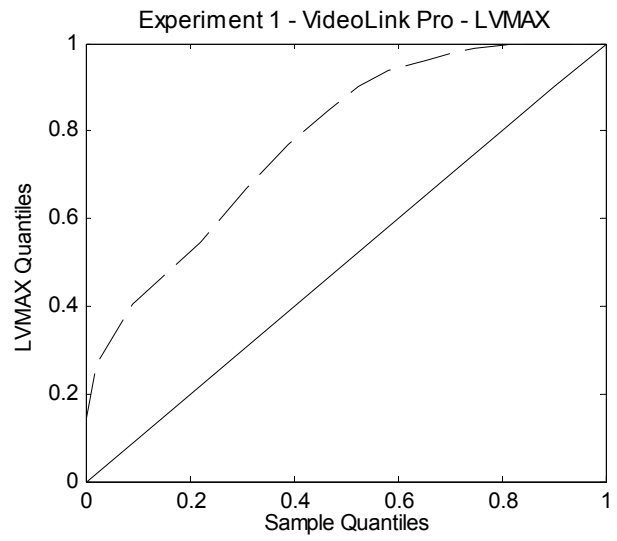


Fig. 6(b)

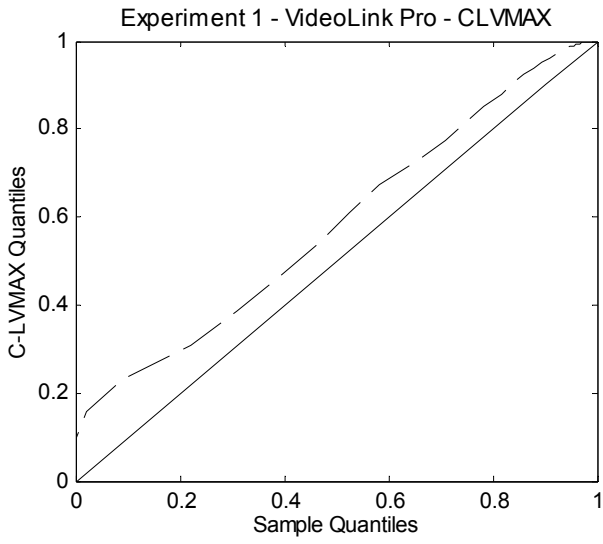


Fig. 6(c)

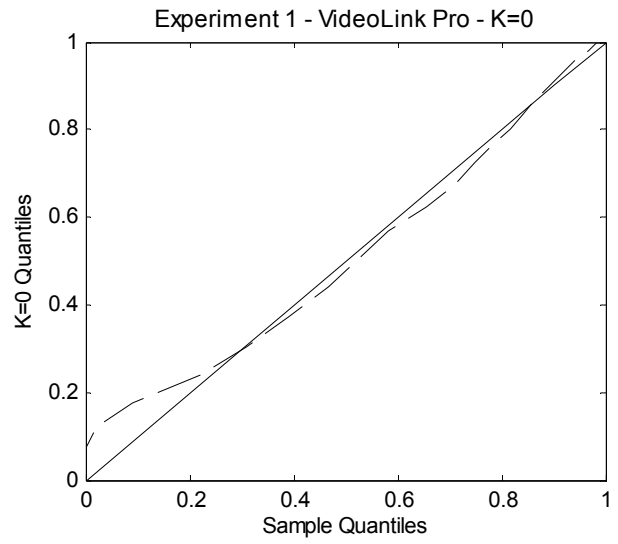


Fig. 6(d)

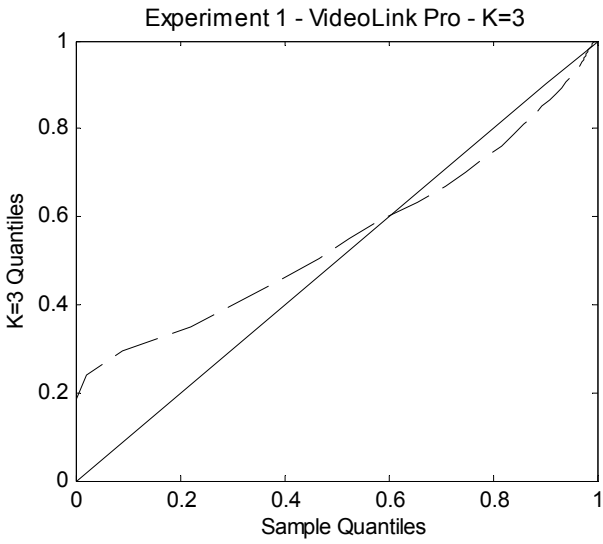


Fig. 6(e)

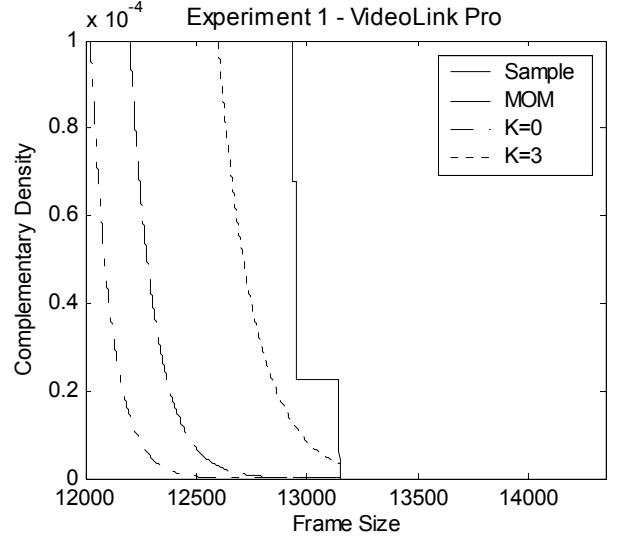


Fig. 6(f)

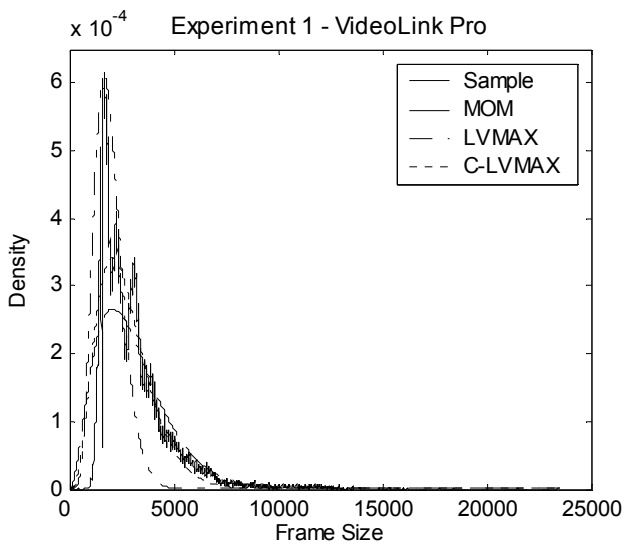


Fig. 6(g)

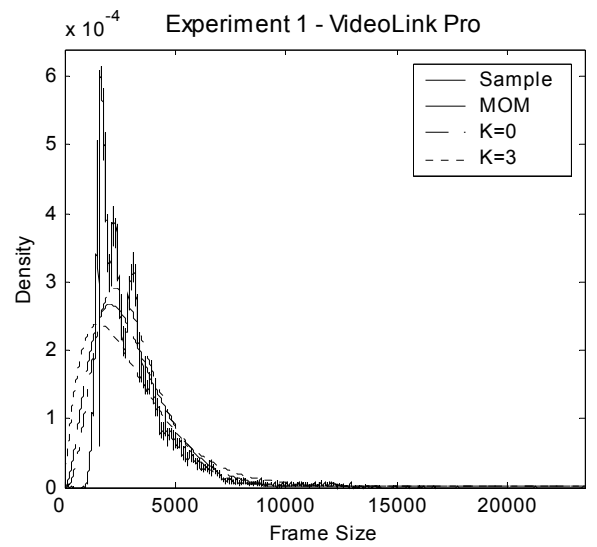


Fig. 6(h)

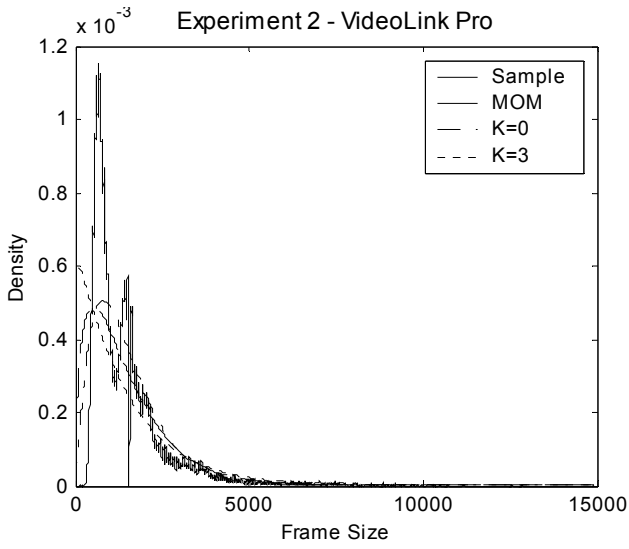


Fig. 6(i)

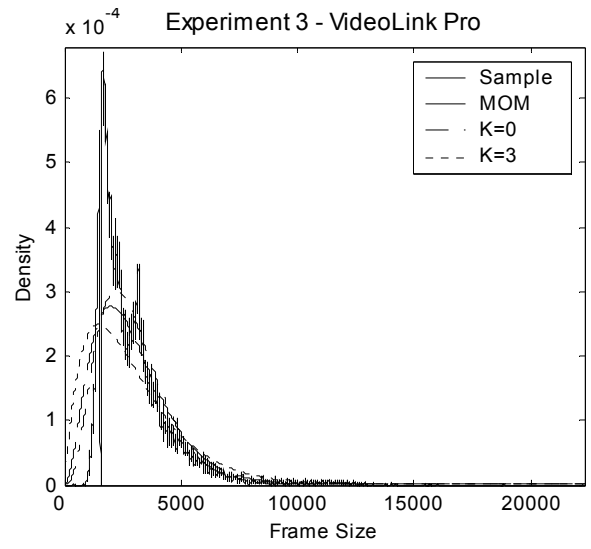


Fig. 6(j)

Figure 6. Frame size histograms-Gamma models, q-q plots and complementary probability functions for terminal VL

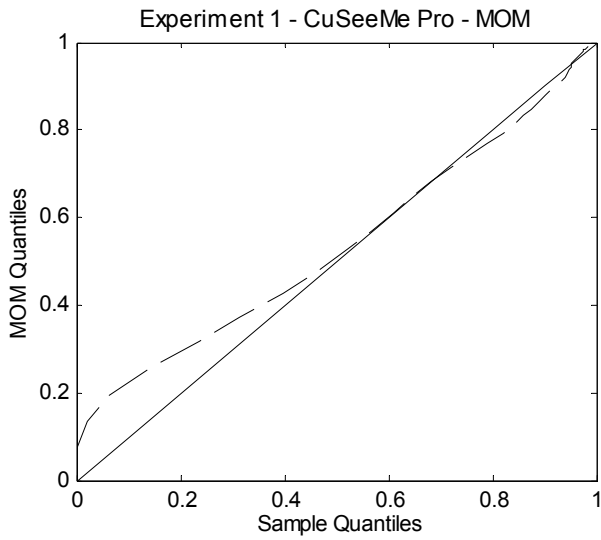


Fig. 7(a)

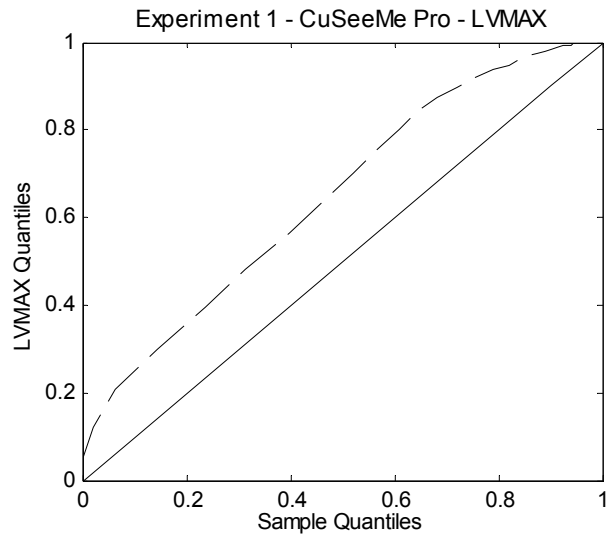


Fig. 7(b)

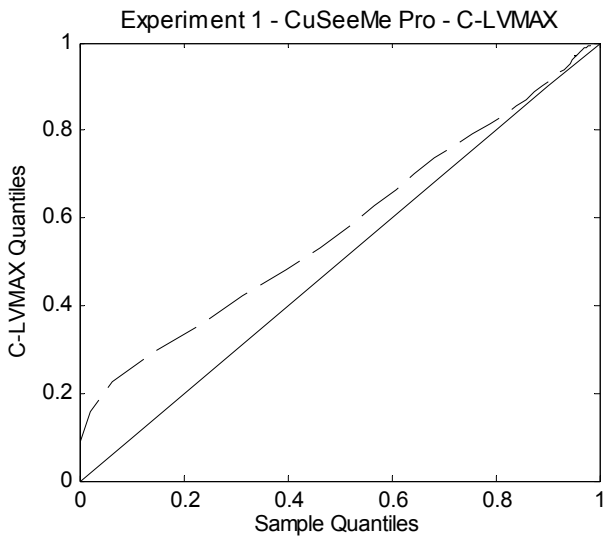


Fig. 7(c)

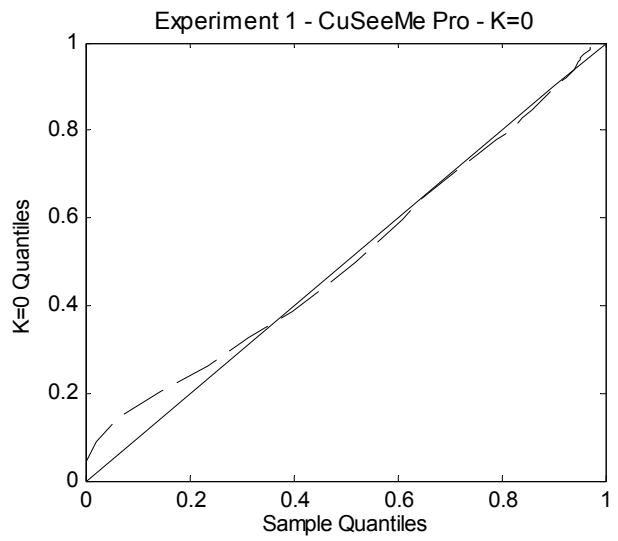


Fig. 7(d)

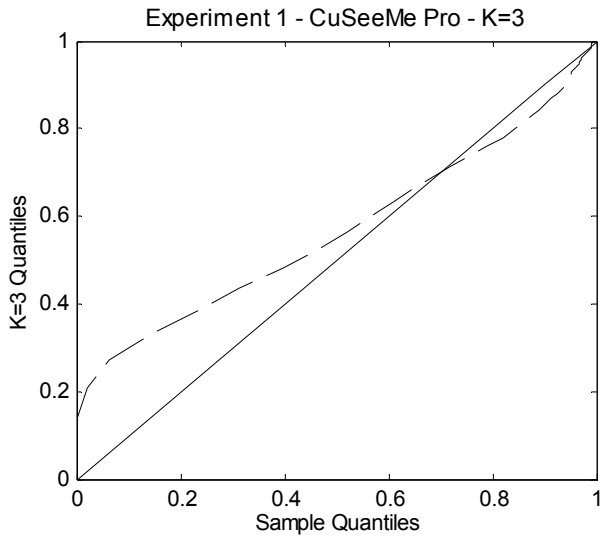


Fig. 7(e)

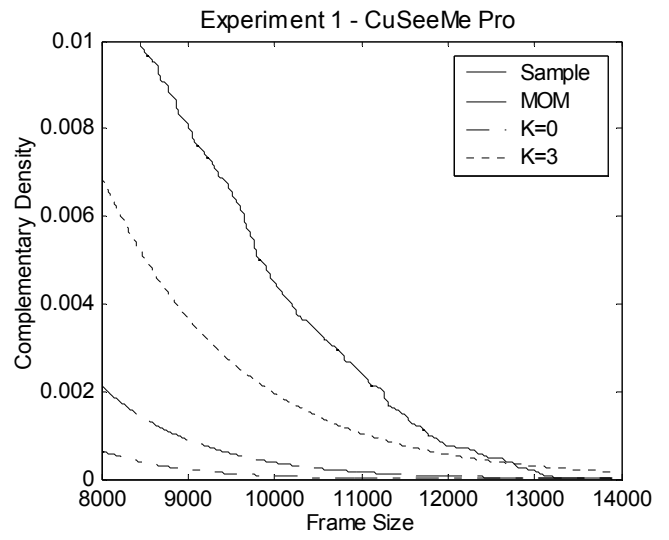


Fig. 7(f)

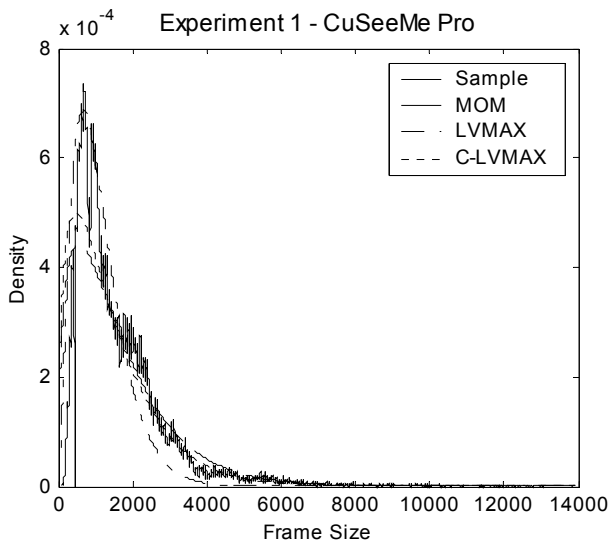


Fig. 7(g)

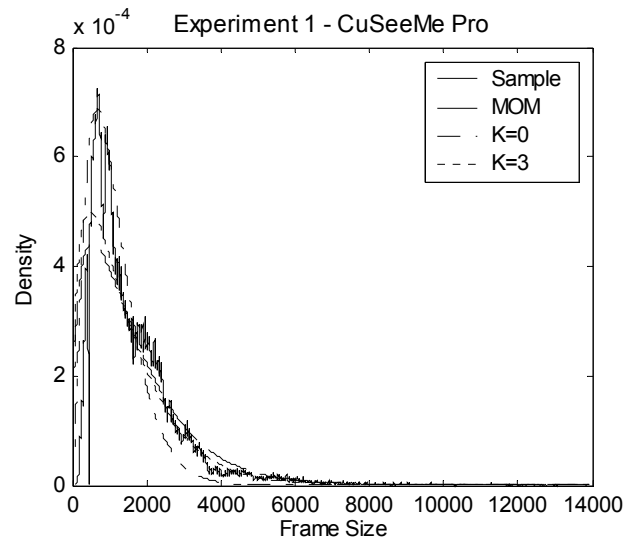


Fig. 7(h)

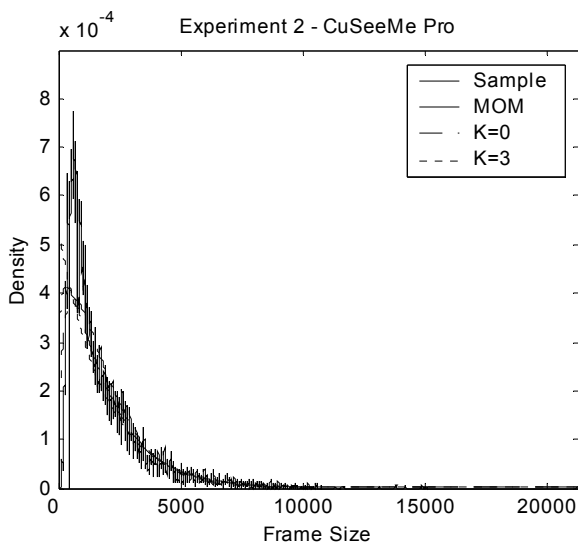


Fig. 7(i)

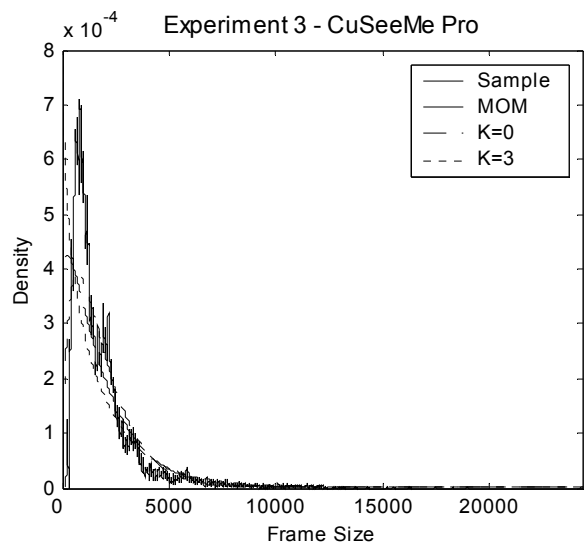


Fig. 7(j)

Figure 7. Frame size histograms-Gamma models, q-q plots and complementary probability functions for terminal CU